Contrast vs non-contrast enhanced microvascular imaging using acoustic sub-aperture processing (ASAP) : in vivo demonstration

Chee Hau Leow[1], Marta Braga[2], Nigel L. Bush[3], Antonio Stanziola[1], Anant Shah[3], Javier Hernández-Gil[2,4], Nicholas J. Long[2,4], Eric O. Aboagye[2], Jeffrey C. Bamber[3], Meng-Xing Tang[1*]

[1]Department of Bioengineering, Imperial College London, UK
[2]Comprehensive Cancer Imaging Centre, Department of Surgery & Cancer,UK
[3]Joint Department of Physics and Cancer Research UK Cancer Imaging Centre, Institute of Cancer Research and Royal Marsden NHS Foundation Trust, UK
[4]Department of Chemistry, Imperial College London, UK
*mengxing.tang@ic.ac.uk

***Abstract*—Angiogenesis plays a vital role in the progression of cancer. Non-invasive imaging techniques capable of assessing the microenvironment are therefore of clinical interest. Although highly sensitive vascular mapping has been demonstrated using ultrafast Power Doppler (PD), the detectability of microvasculature from the background noise may be hindered by the low signal-to-noise ratio (SNR) in deeper region and without the use of contrast agents. We recently developed acoustic sub-aperture processing (ASAP) processing for super-contrast vasculature imaging. This technique relies on the spatial coherence of the backscattered echoes over different acquisitions to substantially reduce the noise floor compared to the power Doppler (PD) technique. In this study, we demonstrate the feasibility of applying ASAP processing for non-contrast enhanced microvascular imaging in preclinical condition, and compare it with contrast enhanced ASAP as well as ultrafast PD. Comparing to PD, ASAP exhibit SNR improvement up to 12 dB. Higher SNR and extra visibility of smaller vessel are also demonstrated in contrast enhanced images in comparison to the non-contrast images. In conclusion, we have demonstrated the feasibility of using ASAP in vivo for non-contrast microvascular imaging, and the added benefit of using contrast agents in microvascular imaging.**

Keywords—noise reduction, high-frame rate ultrasound, Doppler, CEUS, preclinical in-vivo

I. Introduction

Conventional Doppler ultrasound imaging can be used to detect large vessels with relatively fast blood flow [1], [2]. However, the small vessels in the microenvironment is relatively slow and may not be detected using conventional Doppler. For this reason, contrast enhance ultrasound (CEUS) has been established to enhance the flow signal for microvascular imaging and several techniques have been developed to exploit the increase sensitivity and specificity of the injected microbubbles. These include non-linear contrast imaging [3]–[6], non-linear Doppler [7], acoustic angiography [8], and acoustic super-resolution [9], [10].

High frame rate ultrasound further enriched the development of vascular flow imaging with and without the need of contrast agents injection [11]–[15]. Real-time monitoring of the microvasculature is possible with the increased sensitivity of Doppler processing and advanced clutter filtering techniques benefited from the high temporal resolution [11], [16]–[18].

We recently developed a technique known as acoustic sub-aperture processing (ASAP) to improve microvascular imaging using contrast agents [Antonio reference]. This technique relies on the spatial coherence of the backscattered echoes over different acquisition to reduce the background noise in Power Doppler (PD) technique. In this study, our objectives are to demonstrate the feasibility of applying ASAP processing for non-contrast enhanced microvascular imaging, and compare it with contrast enhanced ASAP as well as standard PD.

II. Methods

A. Power Doppler versus Acoustic Sub-Aperture Processing

The signal processing pipelines of PD and ASAP are shown in Fig. 1. In-phase quadrature (IQ) data is reconstructed by applying delay-and-sum to the radio-frequency signal across all channels. A singular value decomposition (SVD) based filter is then applied to remove the tissue clutter and PD image is generated using an autocorrelation estimator estimator [1], [2]:

$$PD = \sum_{t=1}^{T}\sum_{n=1}^{N}|s(n,t)s^{*}(n,t)| \quad (1)$$

where s is the clutter-filtered complex signal, n is the fast time (spatial location) sample index, and t is the slow time (temporal) sample index. The * denotes the complex conjugate and $|-|$ denotes the modulus operator.

With the same receive channel data, two set of IQ-data were reconstructed by splitting the channels into two non-overlapping sub-apertures and cross-correlation estimator is applied to the clutter filtered signals as follow:

$$R = \sum_{T=1}^{t}\sum_{n=1}^{N} s_1(n,t)s_2{}^{*}(n,t) \quad (2)$$

where R is the complex cross-correlated signal, s_1 and s_2 are the clutter-filtered complex signals from the two sub-apertures, n is the fast time sample index, t is the slow time sample index, and * is the complex conjugate operator

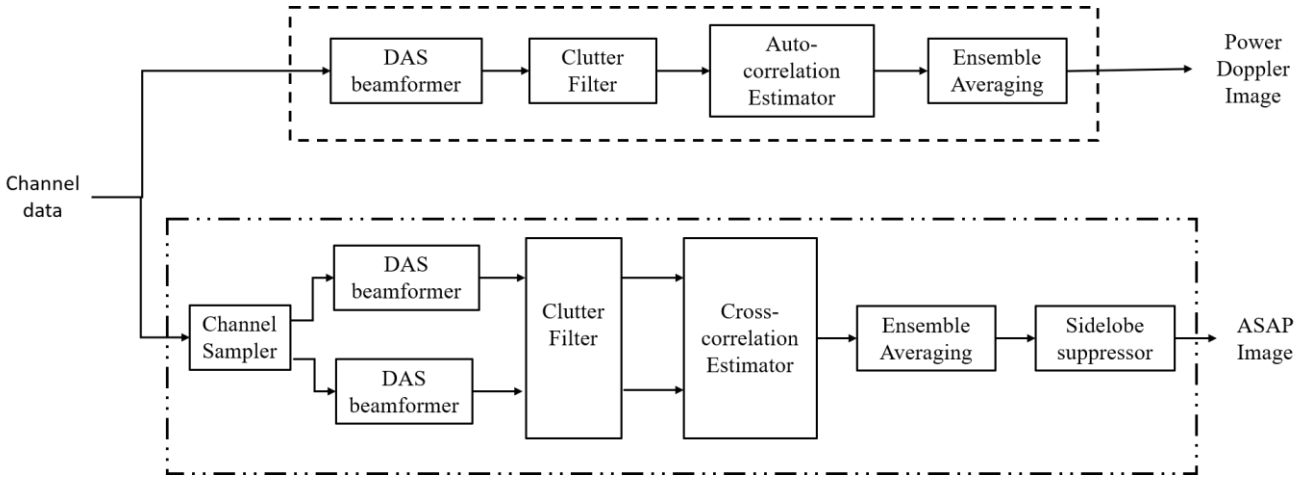

Fig. 1. Signal processing pipelines of Power Doppler and Acoustic sub-aperture processing.

The advantage of the splitting the channel is that the noise in the two independent apertures is not correlated and can be reduced[19]. It should be noted that splitting the channel introduce grating lobe as the pitch between the sub-group of elements increases, however such off -axis signal can be suppressed because the two sub-aperture are independent of each other and the grating lobes are 180 degress out of phase with each other [20]. We therefore introduce a weight vector to suppress the off-axis signals

$$ASAP(n,t) = |R|\, e^{-(\frac{k^2}{k_0{}^2})} \quad (3)$$

where k denotes the phase angle of the sample, and k_o is empirically determined to attenuate out of phase signals at $\pi/3$.

B. *Experimental setup*

In-vivo experiment was conducted as shown in **Fig 2**. A Balb-c mouse was anesthetised via inhalational anaesthetic agents and the body temperature was maintained by a warming pad during the experiment. All procedures complied with the Animals Act 1986 and were approved by the Local Ethical Review Process Committee of Imperial College London.

Mouse kidney was scanned using a L22-14v linear probe mounted on a Verasonics Vantage system (Verasonics Inc., Redmond, WA, USA). Coherent compounded plane wave imaging was performed to collect images at an effective frame rate of 500 Hz. To form an image, fifteen 1-cycle pulses were transmitted at the centre frequency of 18 MHz, spanning the angle range of 15^0. Non-contrast images were first acquired at the mechanical index (MI) of 0.12 whereas contrast images were acquired after the bolus injection of 50ul of home-made microbubbles (10^6 microbubbes/ml) at the MI of 0.05. The experiment was repeated on the second day with higher bubble concentration (10^8 microbubbles/ml).

C. *Data processing and evaluation*

PD and ASAP images were generated as described in the previous section. A graphical processing unit (GPU)-based beamformer was used to accelerate image reconstruction process. The image quality was accessed by comparing the vascular images generated by ASAP and PD. The signal-to-noise ratio (SNR) was quantified as follow:

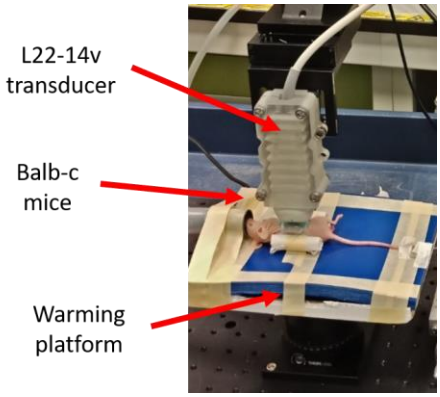

Fig. 2. Experimental setup of the 3D imaging system.

$$SNR = 10\, log_{10}\left(\frac{\mu_s}{\mu_n}\right) \quad (4)$$

where μ_s *and* μ_n are the mean value of the signal and noise region, respectively.

III. Results and Discussion

Fig. 3 shows the comparison between PD and ASAP images of a mouse kidney. Significant background noise is clearly seen in all the PD images. As the background noise is also increasing with the imaging depth, small vessels are barely distinguishable at deeper regions. ASAP, on the other hand, suppressed the background noise and produce high contrast vasculature images. By manually selected the signal (white boxes, Fig. 3) and noise region (green boxes) from both PD and ASAP images, the contrast improvement in terms of SNR are shown in Table I. ASAP is demonstrated to improve the SNR up to 12dB in comparison to PD.

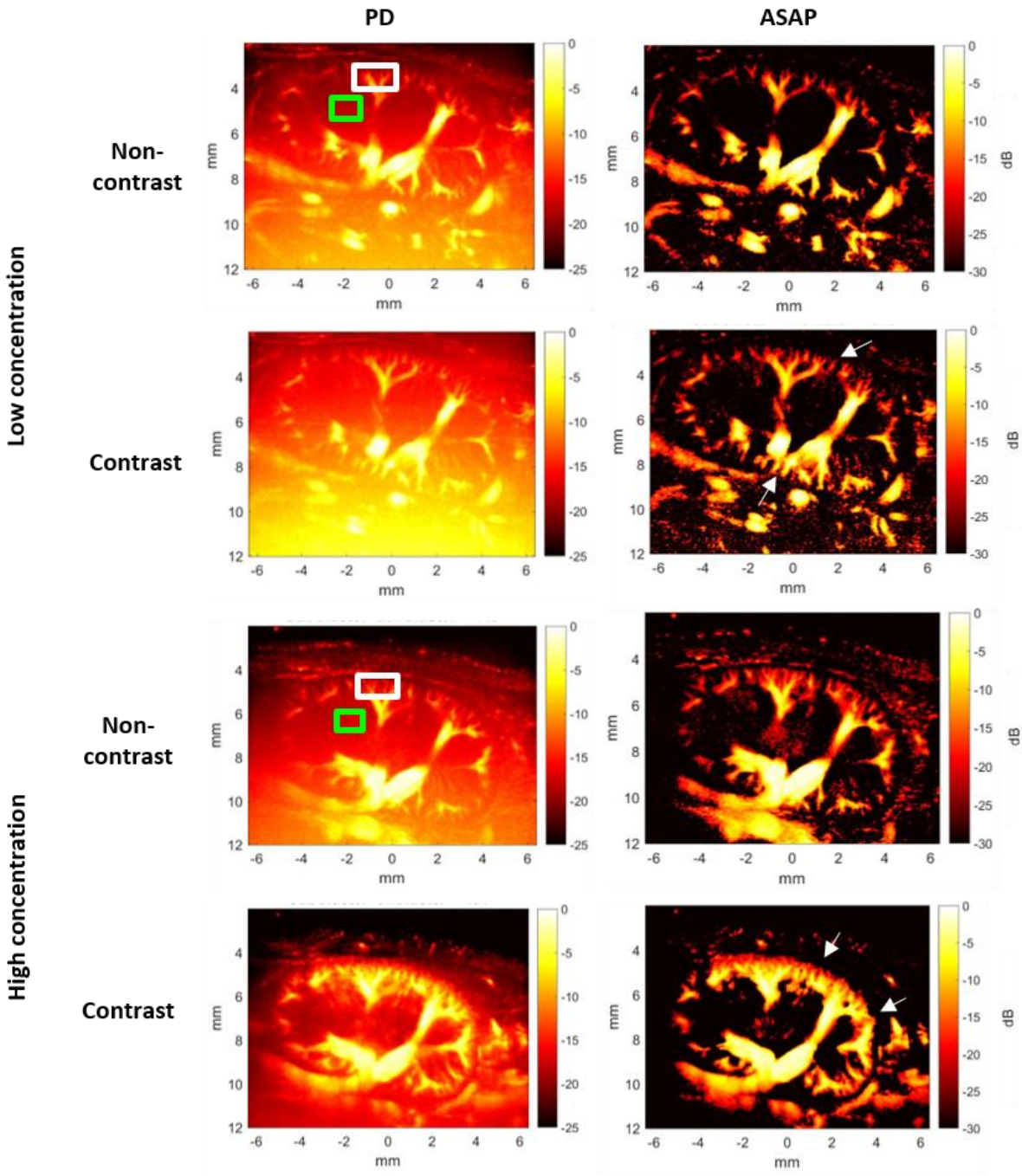

Fig. 3. In-vivo demonstration of mouse kidney processed using Power Doppler (PD) and Acoustic sub-aperture processing (ASAP), with and without contrast.

TABLE I
Comparison of the SNR of the PD and ASAP

Image	SNR (dB)	
	PD	ASAP
Low concentration (10^6 MBs/ml)		
Non-contrast	0.61	9.46
Contrast	0.48	10.71
High concentration (10^8 MBs/ml)		
Non-contrast	0.65	7.34
Contrast	3.65	16.25

* PD = Power Doppler, ASAP= acoustic sub-aperture processing, MBs=microbubbles

Higher SNRs were expected for contrast images than non-contras, and more microvasculature can indeed be seen after contrast injection. (white arrows in Fig 3). Besides, high concentration bolus injection does reveal more vasculature in comparison to the low concentration bolus injection. However, excessive dose of contrast agents may cause acoustic shadowing[21]. It should also be noted that that while the contrast enhanced ASAP would offer more sensitivity to detection of smaller microvasculature and flow, it does require contrast agent injection. Whether to use such contrast enhanced approach should depends on the application, particularly when subtle changes in microvascular information is required in e.g. detection of early changes in angiogenesis.

It should be noted that the ASAP processing has a very similar computational load as PD, and hence has potential to be realised in real-time.

IV. CONCLUSION

In conclusion, we demonstrated the feasibility of using ASAP in vivo for non-contrast microvascular imaging. We also demonstrate the added value of using contrast agents in microvascular imaging.

ACKNOWLEDGMENT

This work is funded by the CRUK Multidisciplinary Project Award (C53470/A22353). C.H Leow would like to acknowledge NVIDIA Corporation for the donation of Titan XP GPU used in this research.

REFERENCES

[1] C. Kasai, K. Namekawa, A. Koyano, and R. Omoto, "Real-time two-dimensional blood flow imaging using an autocorrelation technique," *IEEE Trans Sonics Ultrason*, vol. 32, no. 3, pp. 458–464, 1985.

[2] T. Loupas, J. T. Powers, and R. W. Gill, "An axial velocity estimator for ultrasound blood flow imaging, based on a full evaluation of the Doppler equation by means of a two-dimensional autocorrelation approach," *Ultrason. Ferroelectr. Freq. Control IEEE Trans. On*, vol. 42, no. 4, pp. 672–688, 1995.

[3] F. Lin, S. E. Shelton, D. Espíndola, J. D. Rojas, G. Pinton, and P. A. Dayton, "3-D Ultrasound Localization Microscopy for Identifying Microvascular Morphology Features of Tumor Angiogenesis at a Resolution Beyond the Diffraction Limit of Conventional Ultrasound," *Theranostics*, vol. 7, no. 1, pp. 196–204, Jan. 2017.

[4] R. J. Eckersley, C. T. Chin, and P. N. Burns, "Optimising phase and amplitude modulation schemes for imaging microbubble contrast agents at low acoustic power," *Ultrasound Med. Biol.*, vol. 31, no. 2, pp. 213–219, Feb. 2005.

[5] J. M. G. Borsboom, C. T. Chin, and N. de Jong, "Nonlinear coded excitation method for ultrasound contrast imaging," *Ultrasound Med. Biol.*, vol. 29, no. 2, pp. 277–284, Feb. 2003.

[6] A. Bouakaz, S. Frigstad, F. J. Ten Cate, and N. de Jong, "Super harmonic imaging: a new imaging technique for improved contrast detection," *Ultrasound Med. Biol.*, vol. 28, no. 1, pp. 59–68, Jan. 2002.

[7] D. H. Simpson, C. T. Chin, and P. N. Burns, "Pulse inversion Doppler: a new method for detecting nonlinear echoes from microbubble contrast agents," *Ultrason. Ferroelectr. Freq. Control IEEE Trans. On*, vol. 46, no. 2, pp. 372–382, 1999.

[8] R. C. Gessner, C. B. Frederick, F. S. Foster, and P. A. Dayton, "Acoustic Angiography: A New Imaging Modality for Assessing Microvasculature Architecture," *Int. J. Biomed. Imaging*, vol. 2013, 2013.

[9] K. Christensen-Jeffries, R. J. Browning, M.-X. Tang, C. Dunsby, and R. J. Eckersley, "In vivo acoustic super-resolution and super-resolved velocity mapping using microbubbles," *IEEE Trans. Med. Imaging*, vol. 34, no. 2, pp. 433–440, Feb. 2015.

[10] C. Errico *et al.*, "Ultrafast ultrasound localization microscopy for deep super-resolution vascular imaging," *Nature*, vol. 527, no. 7579, pp. 499–502, Nov. 2015.

[11] J. Bercoff *et al.*, "Ultrafast compound doppler imaging: providing full blood flow characterization," *IEEE Trans. Ultrason. Ferroelectr. Freq. Control*, vol. 58, no. 1, pp. 134–147, Jan. 2011.

[12] J. Jensen, S. Nikolov, A. C. H. Yu, and D. Garcia, "Ultrasound Vector Flow Imaging: II: Parallel Systems," *IEEE Trans. Ultrason. Ferroelectr. Freq. Control*, vol. PP, no. 99, pp. 1–1, 2016.

[13] C. H. Leow, E. Bazigou, R. J. Eckersley, A. C. H. Yu, P. D. Weinberg, and M.-X. Tang, "Flow velocity mapping using high frame-rate plane wave ultrasound and microbubble contrast agents," 2015.

[14] C. H. Leow and M.-X. Tang, "Spatio-Temporal Flow and Wall Shear Stress Mapping Based on Incoherent Ensemble-Correlation of Ultrafast Contrast Enhanced Ultrasound Images," *Ultrasound Med. Biol.*, vol. 44, no. 1, pp. 134–152, Jan. 2018.

[15] M. E. G. Toulemonde *et al.*, "High Frame-Rate Contrast Echocardiography: In-Human Demonstration," *JACC Cardiovasc. Imaging*, 2018.

[16] C. Demené *et al.*, "4D microvascular imaging based on ultrafast Doppler tomography," *NeuroImage*, vol. 127, pp. 472–483, Feb. 2016.

[17] P. Song, A. Manduca, J. D. Trzasko, and S. Chen, "Ultrasound Small Vessel Imaging With Block-Wise Adaptive Local Clutter Filtering," *IEEE Trans. Med. Imaging*, vol. 36, no. 1, pp. 251–262, Jan. 2017.

[18] C. Tremblay-Darveau *et al.*, "Improved contrast-enhanced Power Doppler using a coherence-based estimator," *IEEE Trans. Med. Imaging*, vol. PP, no. 99, pp. 1–1, 2017.

[19] A. Stanziola, C. H. Leow, E. Bazigou, P. D. Weinberg, and M. X. Tang, "ASAP: Super-Contrast Vasculature Imaging using Coherence Analysis and High Frame- Rate Contrast Enhanced Ultrasound," *IEEE Trans. Med. Imaging*, pp. 1–1, 2018.

[20] C. H. Seo and J. T. Yen, "Sidelobe suppression in ultrasound imaging using dual apodization with cross-correlation," *IEEE Trans. Ultrason. Ferroelectr. Freq. Control*, vol. 55, no. 10, pp. 2198–2210, Oct. 2008.

[21] C. F. Dietrich *et al.*, "How to perform Contrast-Enhanced Ultrasound (CEUS)," *Ultrasound Int. Open*, vol. 4, no. 1, pp. E2–E15, Jan. 2018.